NASA TECHNICAL NOTE

NASA TN D-4593

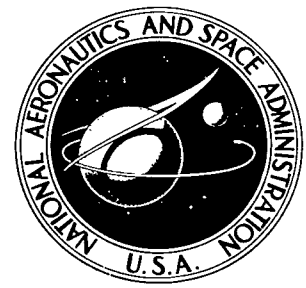

STABILITY ANALYSIS AND MINIMUM THRUST VECTOR CONTROL REQUIREMENTS OF BOOSTER VEHICLES DURING ATMOSPHERIC FLIGHT

by Janos Borsody and Fred Teren

Lewis Research Center
Cleveland, Ohio

NATIONAL AERONAUTICS AND SPACE ADMINISTRATION • WASHINGTON, D. C. • MAY 1968

NASA TN D-4593

STABILITY ANALYSIS AND MINIMUM THRUST VECTOR CONTROL REQUIREMENTS OF BOOSTER VEHICLES DURING ATMOSPHERIC FLIGHT

By Janos Borsody and Fred Teren

Lewis Research Center
Cleveland, Ohio

NATIONAL AERONAUTICS AND SPACE ADMINISTRATION

For sale by the Clearinghouse for Federal Scientific and Technical Information
Springfield, Virginia 22151 – CFSTI price $3.00

ABSTRACT

Generalized analytic results are derived to give a complete description of an open-loop minimal control requirement to maintain stability for a rigid-body vehicle configuration. The results are easily applicable to both pitch and yaw control planes at any flight time of interest by computing some vehicle dependent parameters and evaluating the given equations. The results show that, with good control system design, the deflection requirements can be reduced to about 56 percent of trim deflection. At the same time, because of the method of control, the maximum angle of attack and bending moments can also be substantially reduced.

STAR Category 21

STABILITY ANALYSIS AND MINIMUM THRUST VECTOR CONTROL REQUIREMENTS OF BOOSTER VEHICLES DURING ATMOSPHERIC FLIGHT

by Janos Borsody and Fred Teren

Lewis Research Center

SUMMARY

Open-loop stability boundary conditions are established for a large class of vehicle configurations. The results can be used for preliminary design purposes. The stability boundary is defined as the minimum thrust-vector deflection required to maintain a stable flight. This is accomplished through a fixed-time analysis, which assumes that the basic vehicle parameters remain constant in the time interval of interest. A rigid-body configuration is assumed with uncoupled pitch and yaw control planes. The equations are derived for the pitch plane, but can be applied to the yaw plane with minor modifications. The calculus of variations is used to derive an optimum thrust-vector deflection angle profile with the smallest maximum absolute value, and this control action is used, with minor modifications, to predict the stability boundaries presented.

The results obtained show that the thrust-vector deflection requirements can be reduced to 56 percent of trim requirement with a good closed-loop control system design. The analysis does not include the design of such a system. Attitude response is presented for different wind disturbances and thrust-vector deflection profiles. These results indicate rapid convergence and divergence of attitude error for control capability above or below the stability boundary value, respectively.

INTRODUCTION

Most present booster vehicles use thrust vectoring for control. This may be accomplished in one of several ways, but the most common method is to gimbal the engine or engines. For liquid-fueled rockets, this method is used almost exclusively. However, thrust-vector deflection (TVD) of solid-fueled motors presents problems not encountered

with liquid-fueled engines. It is not feasible to gimbal the entire motor, and, if only the nozzle portion is gimballed, severe seal and actuator problems are encountered. Secondary fluid injection has been shown to be an effective steering technique, but, for many vehicle requirements, it leads to increased complexity, large injectant requirements, and reduced payload capability. Furthermore, any steering which is accomplished by generating side forces near the base of the vehicle introduces large bending moments in the vehicle structure in flying through winds. Some of the difficulties associated with TVD can be overcome by the use of active or passive aerodynamic surfaces, but these techniques encounter other difficulties especially with regard to size, location, control, and integration with TVD or reaction steering devices. It is apparent that important design and performance problems are encountered when vehicle control is provided by either TVD, reaction, or aerodynamic means. Therefore, it is important to define realistic steering requirements for solid-propellant rocket vehicles so that optimum control system configurations can be established.

Minimum control requirements will be derived by assuming that the control force is obtained by thrust deflection. It should be noted, however, that the simplified analysis can be applied directly to active aerodynamic surfaces or reaction control devices. Because these control devices are located ahead of the center of gravity, they tend to reduce sideslip, which improves the accuracy of the simplified analysis.

In the past, TVD requirements have been established by simulating the vehicle flight through a family of winds and noting the maximum thrust deflection angle used (ref. 1). Most present-day vehicles use conventional control systems that utilize attitude and attitude rate feedback. They are designed to trim the vehicle during powered flight, that is, to maintain the nominal flight attitude even in the presence of winds. Until the development of solid-fueled engines, TVD angle was not a limiting factor and most control systems were designed for trim deflection requirements. Solid-fueled engines pose problems in obtaining TVD, which make it desirable to reduce the deflection requirements.

The purpose of this report is to establish the TVD stability limits for a rigid-body configuration and a family of expected flight winds. A stable vehicle will be defined as one which can be returned to its desired flight path by appropriate control action when it deviates as a result of some disturbance. From the previous definition, the stability limit will be the minimum control action necessary to return the vehicle to its desired flight path after the disturbance subsides. The mathematical derivation of this stability limit is given in the analysis. Various assumptions are made to simplify the mathematical model in order to give a closed-form solution. These assumptions and their effect on the results are discussed in the analysis.

Validity of the theoretical results is established by detailed six degrees of freedom

(rigid body) computer simulations for two representative vehicle configurations: an intermediate solid booster (260 in. (660 cm) solid) and a large solid vehicle capable of putting one million pounds of payload into 100-nautical-mile (184-km) circular orbit. The required propulsion, aerodynamic, and weight data for these vehicles are based on a preliminary design study conducted at Lewis Research Center. The results include curves of theoretical and actual (detailed computer simulation) stability limits, and attitude error convergence and divergence rates for TVD capability above and below the stability limit, respectively. The computer simulation and theoretical results are based on simplified wind shapes to reduce mathematical complexity, although the theory is applicable to any wind profile.

ANALYSIS AND ASSUMPTIONS

The equations of motion will be derived for a rigid-body configuration in order to simplify the analysis and to make the results easily applicable to vehicles of different size and aerodynamic behavior. The vehicle is assumed to have axial symmetry with negligible coupling between pitch and yaw planes. This allows independent pitch or yaw plane analysis. Thus the results of this report may not apply to vehicles with large wing sections or to vehicles having large coupling between pitch and yaw planes.

The equations of motion are derived in a local horizontal, Cartesian coordinate system whose origin is located at the vehicle's center of gravity. Aerodynamic moments are cancelled by thrust deflection. Because the duration of maximum flight winds is generally shorter than the atmospheric flight time, the analysis will be restricted to a time interval in which trajectory and vehicle parameters remain constant. Thus, the equations may be used to analyze vehicle response at any desired flight time. The results in this report are given for maximum aerodynamic loading, which, in general, occur near maximum dynamic pressure. In order to obtain conservative control requirements, maximum wind velocity and wind shear (the rate of change of wind speed with altitude) are assumed to coincide with maximum dynamic pressure.

With these simplifying assumptions, there are two independent variables left in the problem, namely, wind velocity profile and control action against time. For statistically predictable winds (if the flight wind can be predicted in advance), the maximum control requirements could be reduced by using more control action in the low-wind velocity region than that required to trim the vehicle. This causes the vehicle to turn into the direction of high wind, thus reducing the angle of attack and, consequently, the control requirements in the high-wind region. In effect, the control requirement is averaged over a longer period of time, and the peak requirement is reduced. This control scheme has the possible shortcoming of building up too high an angle of attack due to excess control

before the high-wind-velocity region is encountered, which will limit the maximum control that can be used. With this consideration in mind, it is desired to determine how much can be gained by using maximum-control capability as soon as possible in the low-wind region, in other words, what percent of trim control is needed to maintain stability. The main purpose of this report is to obtain the theoretical minimum-control requirements applicable for most vehicle configurations. To this end, a general closed form stability boundary condition will be established. This has the form of an integral relation between the wind distribution and the necessary control action which will ensure a stable flight. The control system will be assumed to operate open loop; no attempt is made to design a closed-loop system. To illustrate how this generalized stability equation may be applied, the stability boundary will be derived for two different wind profiles and control actions.

Derivation of General Stability Condition

The following discussion includes the derivation of general stability boundary limit. To illustrate the usefulness of this result, specific boundary limits will be derived for rectangular and triangular wind profiles. The analysis is carried out for a rigid-body configuration with the assumption of uncoupled control planes; that is, the pitch and yaw planes do not interact. Figure 1 shows the basic vehicle configuration and the parameters employed in the analysis. The variables used are defined in appendix A. The vehicle is assumed to be aerodynamically unstable with thrust-vector control for stabilization. The reference trajectory is a zero angle-of-attack flight. The basic vehicle equations of motion are given in appendix B. The principal analytic results can be derived from the moment equation

$$\sum M_{CG} = I\ddot{\Theta} = N l_a \alpha - T l_c \delta \qquad \text{(B2c)}$$

This equation applies for small deflection angles and a normal force that is proportional to the angle of attack.

Nominal trajectory. - The nominal flight is a no wind, zero angle of attack (or zero lift) trajectory, which defines the nominal flight profile, and pitch attitude (Θ_n). The nominal flight parameters are

$$\alpha_n = 0$$

$$\alpha_{wn} = 0$$

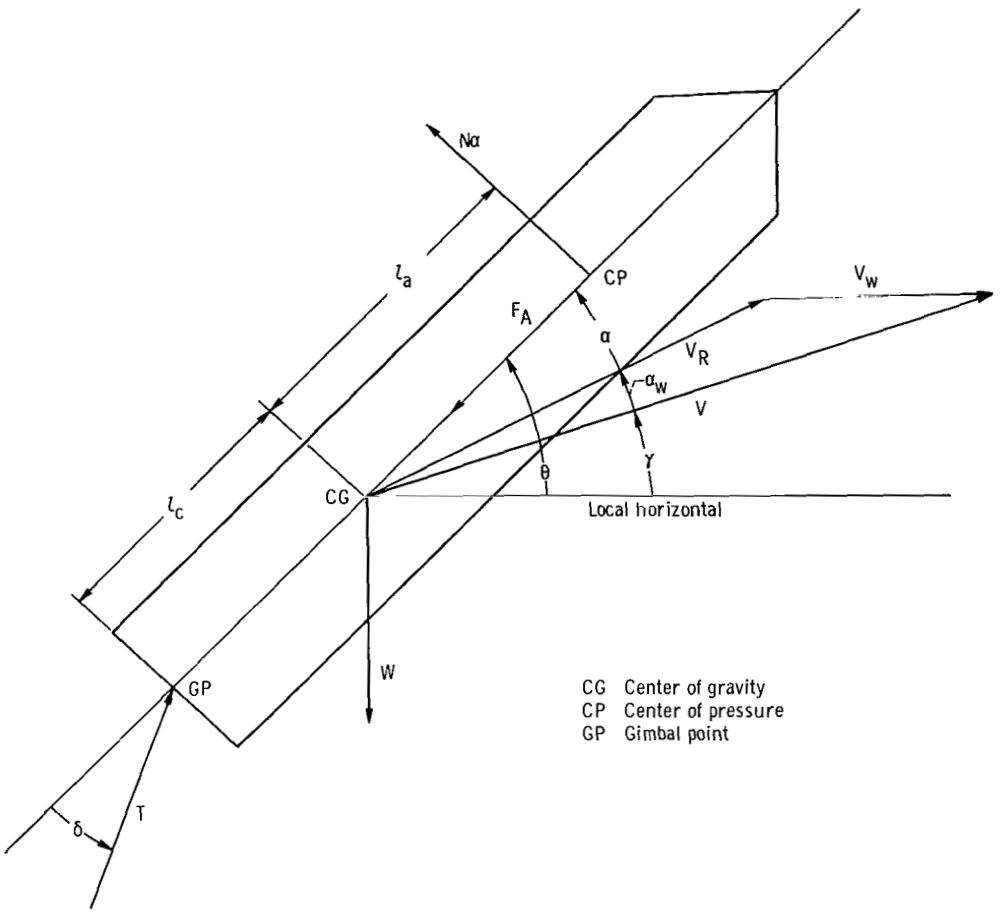

Figure 1. - Basic vehicle configuration.

Then, from equation (B1f), the nominal flight path angle is given by

$$\gamma_n = \Theta_n$$

From equation (1)

$$\delta_n = -\frac{I\ddot{\Theta}_n}{T l_c} \tag{1}$$

This nominal gimbal angle requirement is largest during pitch-over, that is, the time interval immediately after the vertical rise maneuver, which occurs before the high-wind velocity region. Because the gimbal requirements due to winds at maximum aerodynamic load conditions are much larger than the initial pitch-over gimbal requirement, this por-

tion of the flight poses no control problem. Also, the nominal control requirements in the high-wind region are very small, thus their contribution to the overall TVD angle is small. Therefore, the portion of the powered flight that can encounter stability problems due to deflection limitations is the high-wind velocity or maximum dynamic pressure region.

Trim case. - The flight is trimmed if the aerodynamic moments are instantaneously cancelled by thrust deflection (this assumes an ideal autopilot). This will force the vehicle to maintain the nominal flight attitude (Θ_n) even in the presence of winds: $\Theta_T = \Theta_n$. However, the vehicle position in an inertial coordinate system will deviate due to sideslip. Sideslip is the integrated effect of acceleration due to aerodynamic forces and the thrust component necessary to cancel the aerodynamic moments. From equation (B1c)

$$\delta_T = -\frac{I\ddot{\Theta}_n}{T l_c} + \frac{N l_a}{T l_c}\alpha_T$$

Substituting equation (1) into this equation gives

$$\frac{\delta_T - \delta_n}{\alpha_T} = \frac{N l_a}{T l_c} \equiv B \tag{2}$$

The parameter B determines gimbal requirements for trim. One of the purposes of this report is, then, to determine how much this trim gimbal requirement can be reduced while still maintaining stability. The trim angle of attack using equation (B1f) is given by

$$\alpha_T = -(\gamma_T - \gamma_n) - \alpha_w \tag{3}$$

If the variation in flight path angle is assumed to be negligible, the trim deflection is proportional to the angle of attack due to wind, thus equation (2) gives a simple formula to calculate trim deflection.

Stability criteria. - In order to maintain a vehicle on some desired flight path, a certain amount of control action is required to counterbalance aerodynamic disturbances. A trimmed vehicle is by definition stable. The question that arises is what happens to a vehicle with a given control capability (δ_{max}) which is smaller than the trim control requirement for a given wind disturbance? There are two possibilities: The vehicle may lose control; that is, the attitude error ($\Theta - \Theta_n$) increases indefinitely. Or the vehicle may return to the desired flight path after the disturbance ceases; that is, the attitude error increases, then goes to zero. In this report, the vehicle will be considered stable if it maintains the desired flight path or if it returns to the desired flight path after it has deviated due to some disturbance. The stability boundary is the minimum control action

necessary for stability divided by $B\alpha_{w,max}$. In general, the maximum trim deflection requirement is given by $B\alpha_{T,max}$. However, if the trajectory does not drift, then $\alpha_{T,max} = -\alpha_{w,max}$ (as shown by eq. (3)), and the trim deflection requirement becomes $B\alpha_{w,max}$. The stability boundary obviously is a function of the vehicle parameters and the wind duration and shape. The mathematical definition of stability is given by

$$\lim_{t\to\infty} (\Theta - \Theta_n) = 0 \tag{4a}$$

From this equation the stability boundary can be obtained.

The solution of $(\Theta - \Theta_n)$ contains exponential terms, whose coefficients are equal to the residues of the Laplace transform of $(\Theta - \Theta_n)$. In order for $(\Theta - \Theta_n)$ to have a stable solution, the residues of the unstable modes of $(\Theta - \Theta_n)$ must all be zero; that is,

$$\lim_{s\to\beta_i} (s - \beta_i)\mathcal{L}(\Theta - \Theta_n) = 0 \qquad \text{for } i = 1, 2, \ldots, N \tag{4b}$$

where β_i are the unstable modes. This equation gives the general stability boundary; its application will be given in the following paragraphs.

It can easily be shown that, if the $\mathcal{L}(\Theta - \Theta_n)$ has the form

$$\mathcal{L}(\Theta - \Theta_n) = \frac{1}{D(s)}\left[N_1(s)\mathcal{L}(\delta - \delta_n) + N_2(s)\mathcal{L}(\alpha_w)\right]$$

where N_1, N_2, and D are polynomials in s, and β_i are the unstable roots of D, the stability condition can be expressed as

$$\mathcal{L}(\delta - \delta_T) = 0$$

at $s = \beta_i$ for $i = 1, 2, \ldots, N$. This equation may be used if the trim deflection profile and the β_i are available.

Simplified Stability Analysis

To simplify the moment balance equation (eq. (B3)), it is assumed that the flight-path angle is insensitive to winds and control action; that is, $\gamma = \gamma_n = \gamma_T$. With this assumption, the moment balance equation of appendix B becomes

$$\mathcal{L}(\Theta - \Theta_n) = -\frac{\frac{\beta^2}{B}}{s^2 - \beta^2}\,\mathcal{L}\left[(\delta - \delta_n) + B\alpha_w\right] \tag{5}$$

The finiteness of $\delta - \delta_n$ and α_w assure that their transforms cannot have poles in the right half of the plane, thus, the only possible unstable mode is located at $s = \beta$. Applying the stability boundary condition of equation (4b) gives

$$\lim_{s\to\beta} \mathcal{L}(\delta - \delta_n) = -B \lim_{s\to\beta} \mathcal{L}(\alpha_w) \tag{6a}$$

or

$$\int_0^\infty e^{-\beta t}(\delta - \delta_n)\, dt = -B \int_0^\infty e^{-\beta t}\alpha_w\, dt \tag{6b}$$

This equation is one of the important analytical results of this report. It gives an integral relation between any wind history and the corresponding gimbal-angle requirement for stable vehicle control. To show how this equation is applied, two particular wind profiles will be considered with two different control schemes.

Rectangular wind. - The wind is assumed to be a rectangular pulse of duration τ and amplitude $\alpha_{w,max}$. For control, assume that the thrust is instantaneously deflected, as soon as the wind is observed, to its maximum value δ_{max}. Sketch (a) gives a pictorial representation of both wind and control.

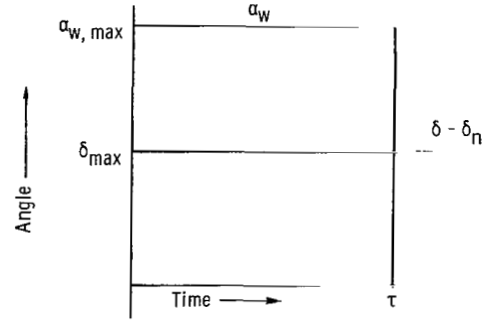

(a)

Using equation (6b) yields

$$\delta_{max}\int_0^{\infty} e^{-\beta t}\,dt = -B\alpha_{w,\,max}\int_0^{\tau} e^{-\beta t}\,dt$$

or

$$-\frac{\delta_{max}}{B\alpha_{w,\,max}} = 1 - e^{-\tau\beta}$$

The quantity $-\delta_{max}/B\alpha_{w,\,max}$ is defined to be the boundary limit. It is approximately equal to the thrust deflection required for stability divided by the maximum trim deflection required. The formula is exact, as shown in the following equation, if the flight-path angle is unchanged from the nominal to the perturbed flight.

$$y_{BR} = 1 - e^{-\tau\beta} \tag{7}$$

Therefore,

$$y_{BR} = -\frac{\delta_{max}}{B\alpha_{w,\,max}} \tag{8}$$

Using equations (2) and (3), the boundary can be written as

$$y_{BR} = \frac{\delta - \delta_n}{\delta_T - \delta_n}$$

The results of equation (8) are plotted in figure 2. For the vehicles considered, β is between 0.4 and 0.6 radian per second. For large winds, the wind duration is at least 10 seconds; therefore, $\tau\beta \geq 4$. For these values of $\tau\beta$, the decrease in gimbal requirements from the trim value is negligible or zero so that full trim control would be required to maintain stability when rectangular wind profiles are encountered. Fortunately, large rectangular wind profiles are not encountered.

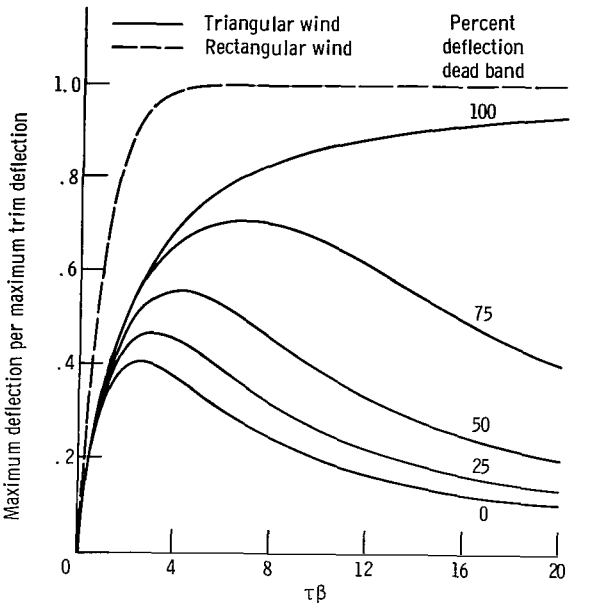

Figure 2. - Theoretical stability boundary without flight-path angle effect.

In order to obtain the attitude response to rectangular winds, the inverse Laplace transform of equation (5) must be evaluated. Define

$$u(t - x) = \begin{cases} 0 & \text{for } 0 \leq t < x \\ 1 & \text{for } x \leq t \end{cases} \quad x \text{ positive}$$

then

$$\delta - \delta_n = \delta_{max} u(t)$$

$$\alpha_w = \alpha_{w,max}[u(t) - u(t - \tau)]$$

Taking the Laplace transform and substituting into equation (5) gives

$$\mathcal{L}(\Theta - \Theta_n) = -\frac{\frac{\beta^2}{B}}{s^2 - \beta^2} \frac{1}{s}\left[\delta_{max} + B\alpha_{w,max}(1 - e^{-\tau s})\right]$$

The inverse transform is given by

$$\frac{\Theta - \Theta_n}{-\alpha_{w,max}} = (1 - y_{BR})\left[\cosh \tau\beta\left(\frac{t}{\tau}\right) - 1\right]u(t) - \left[\cosh \tau\beta\left(\frac{t}{\tau} - 1\right) - 1\right]u\left(\frac{t}{\tau} - 1\right) \quad (9)$$

Triangular wind. - In this section, the wind is assumed to be triangular, which closely approximates synthetic winds often used in preliminary design studies. For control action, assume that the vehicle is trimmed until time (t = a), then apply maximum control capability.

At time t = a, the thrust deflection is equal to K times the maximum gimbal capability. This corresponds to a dead-band in gimbal deflection of $K\delta_{max}$, within which the vehicle is to be trimmed. Outside this band, maximum control is used, thus a is given by

$$a = -\frac{\delta_{max}}{B\alpha_{w,max}} \frac{\tau}{2} K \quad (10)$$

where δ_{max} and $\alpha_{w,max}$ are the maximum deflection requirement and maximum wind angle of attack, respectively.

Referring to equation (7), a becomes

$$a = y_{BR} \frac{\tau}{2} K \quad (11)$$

Sketch (b) gives a pictorial representation of the control action and wind profile.

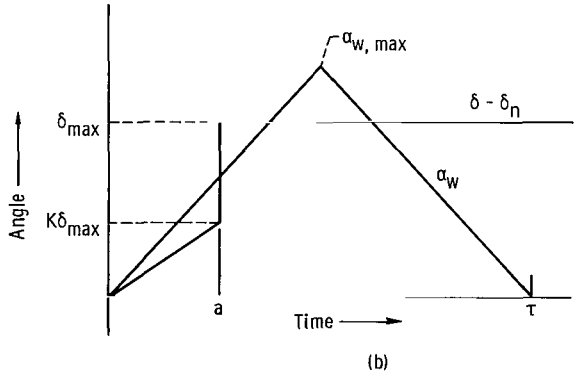

(b)

Using equations (2) and (3), the control action is given by

$$\delta - \delta_n = \begin{cases} B\alpha_T \simeq -B\alpha_w & \text{for } 0 \le t < a \\ \delta_{max} & \text{for } a \le t \end{cases}$$

or

$$\delta - \delta_n = -B[u(t) - u(t - a)]\alpha_w + \delta_{max}u(t - a)$$

where α_w is given by

$$\alpha_w = \frac{\alpha_{w,max}}{\frac{\tau}{2}}\left[u(t)t - 2u\left(t - \frac{\tau}{2}\right)\left(t - \frac{\tau}{2}\right) + u(t - \tau)(t - \tau)\right]$$

Taking the Laplace transforms and applying the boundary condition given by equation (6a) result in the stability boundary

$$\left[1 - \frac{\tau\beta}{2}y_{BR}(1 - K)\right]e^{-(\tau\beta/2)y_{BR}K} = e^{-\tau\beta}\left(2e^{\tau\beta/2} - 1\right) \tag{12}$$

The results of this equation are also plotted in figure 2. For $\tau\beta = 4$ and 100-percent deflection dead band, the reduction in deflection requirement from the trim value is approximately 31 percent. For smaller values of deflection dead band, the reduction is much greater. For a 0-percent deflection dead band, the maximum reduction is 62 percent of trim value.

Substituting $\mathscr{L}(\delta - \delta_n)$ and $\mathscr{L}(\alpha_w)$ into equation (5) and taking the inverse Laplace transform give the attitude response to triangular winds in terms of the boundary condition; that is,

$$\frac{\Theta - \Theta_n}{-\alpha_{w,max}} = \frac{2}{\tau\beta}\left(u\left(\frac{t}{\tau} - 1\right)\left[\sinh\tau\beta\left(\frac{t}{\tau} - 1\right) - \tau\beta\left(\frac{t}{\tau} - 1\right)\right] - 2u\left(\frac{t}{\tau} - \frac{1}{2}\right)\left[\sinh\tau\beta\left(\frac{t}{\tau} - \frac{1}{2}\right) - \tau\beta\left(\frac{t}{\tau} - \frac{1}{2}\right)\right] + u\left(\frac{t}{\tau} - y_{BR}\frac{K}{2}\right)\left\{\sinh\tau\beta\left(\frac{t}{\tau} - y_{BR}\frac{K}{2}\right) - \tau\beta\left(\frac{t}{\tau} - y_{BR}\frac{K}{2}\right) - y_{BR}\frac{\tau\beta}{2}(1 - K)\left[\cosh\tau\beta\left(\frac{t}{\tau} - y_{BR}\frac{K}{2}\right) - 1\right]\right\}\right) \tag{13}$$

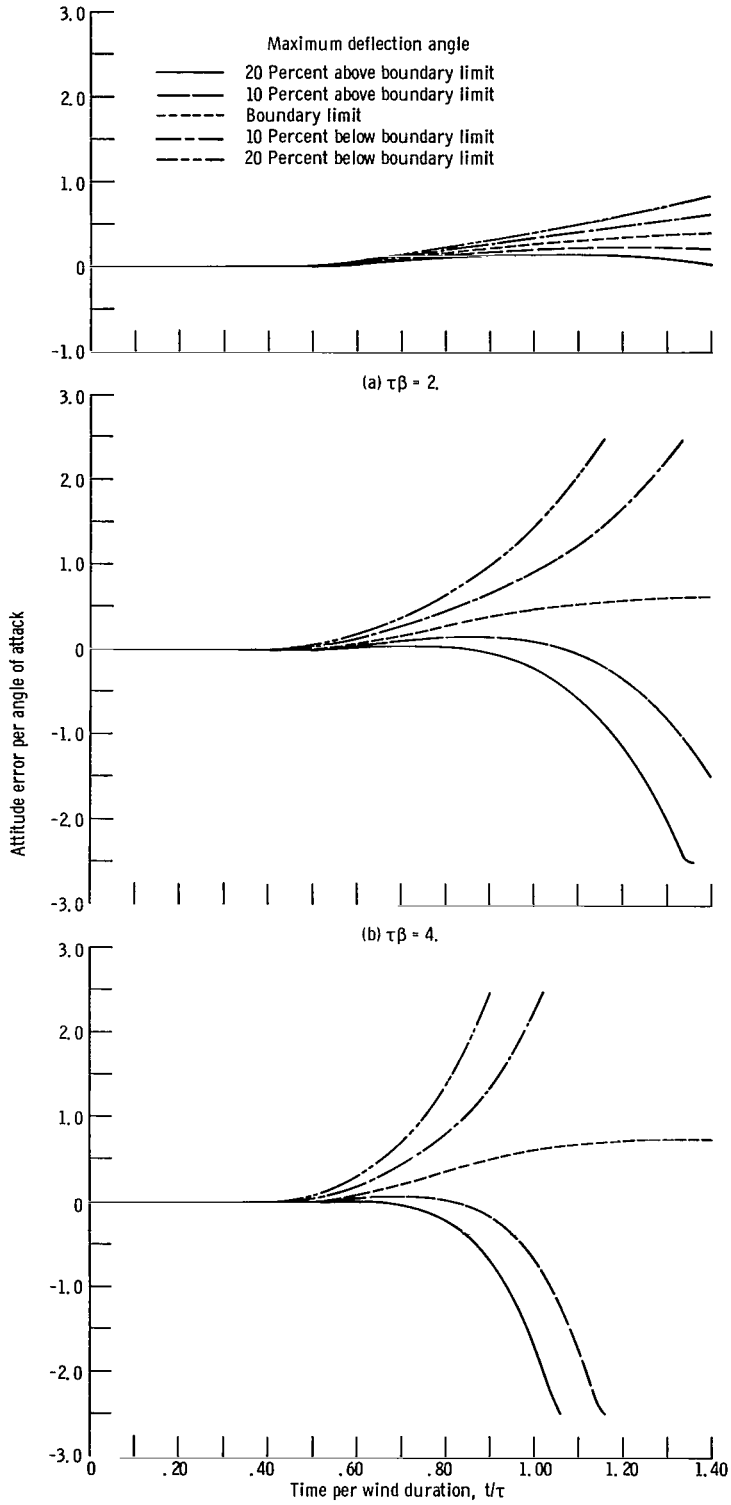

(a) $\tau\beta = 2$.

(b) $\tau\beta = 4$.

(c) $\tau\beta = 6$.

Figure 3. - Simplified analytic attitude error convergence and divergence rates. No flight-path angle effect; deflection dead band, 100-percent.

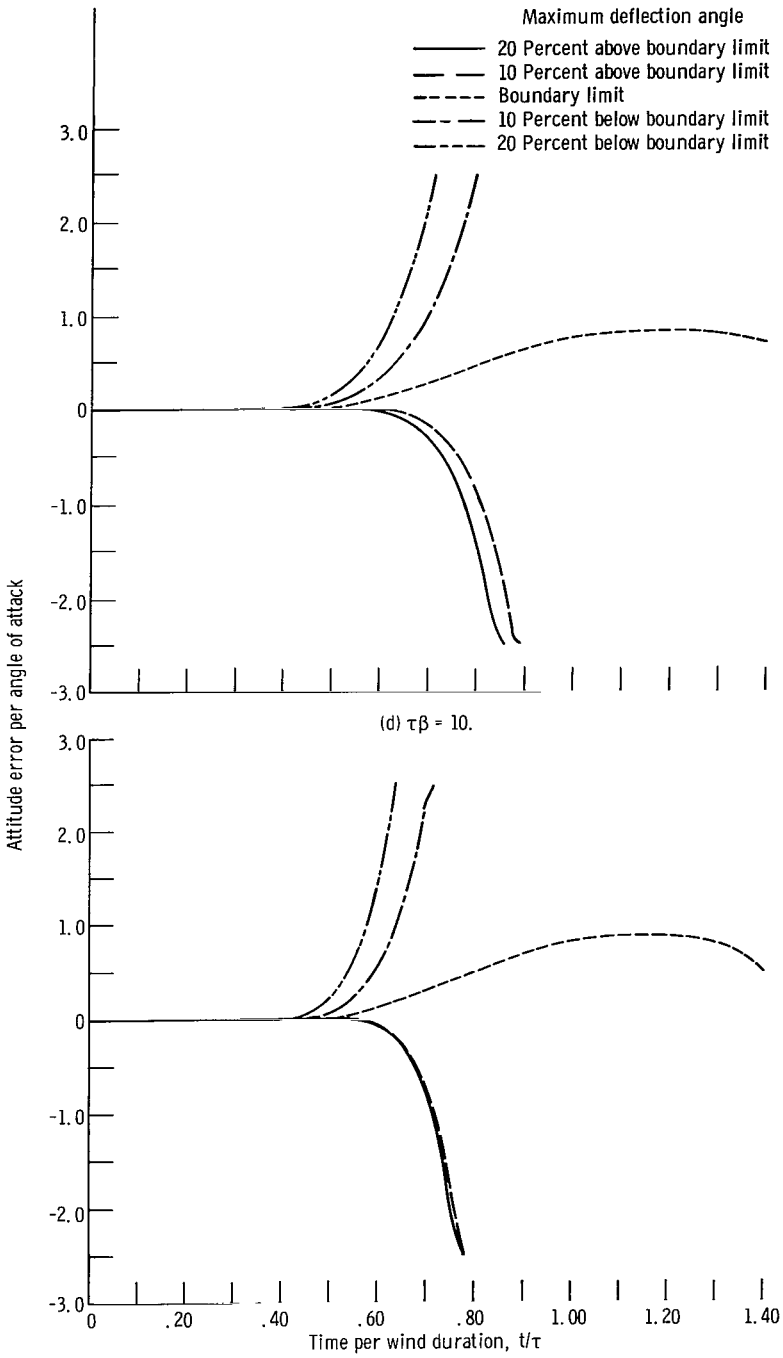

(d) $\tau\beta = 10$.

(e) $\tau\beta = 14$.

Figure 3. - Concluded.

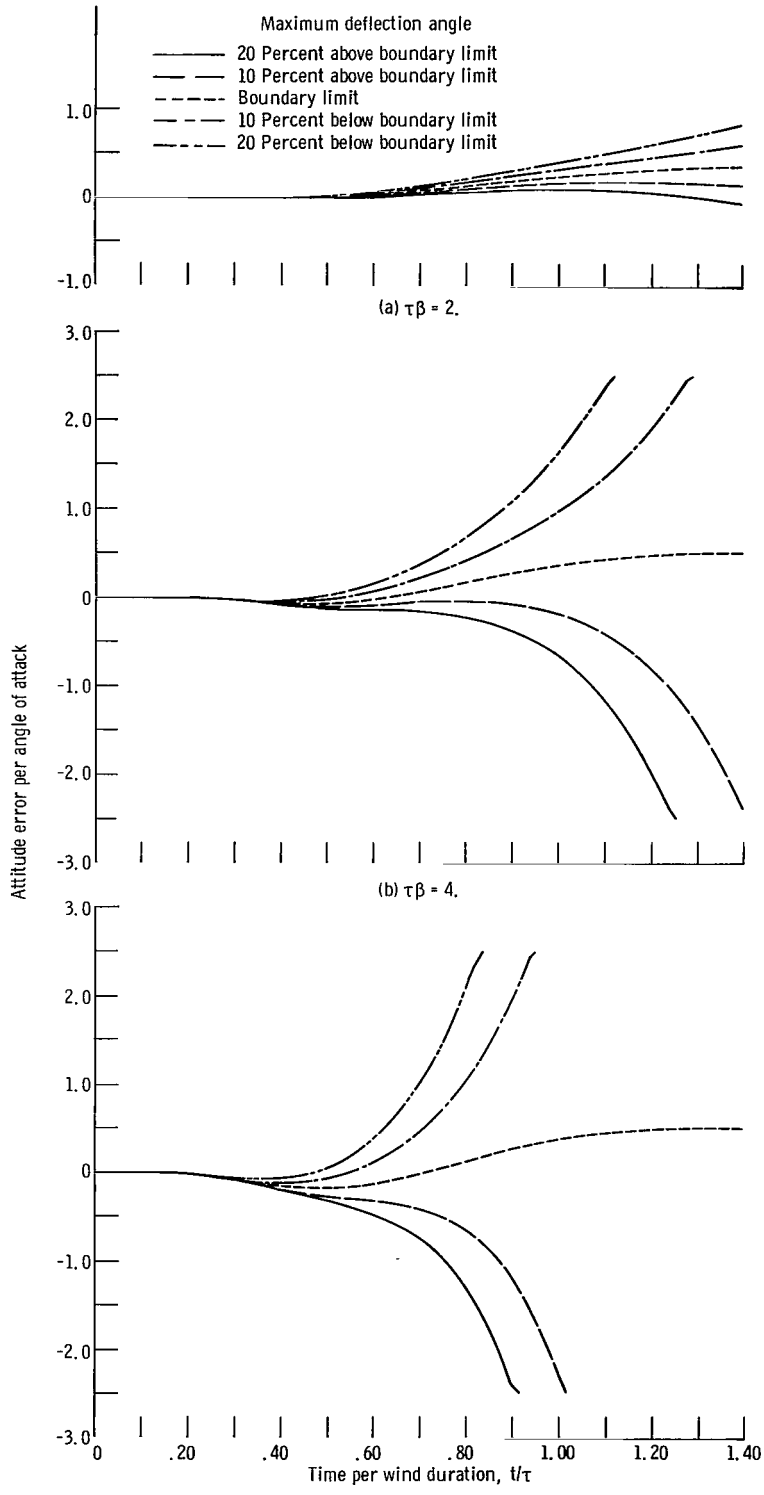

Figure 4. - Simplified analytic attitude error convergence and divergence rates. No flight-path angle effect; deflection dead band, 50 percent.

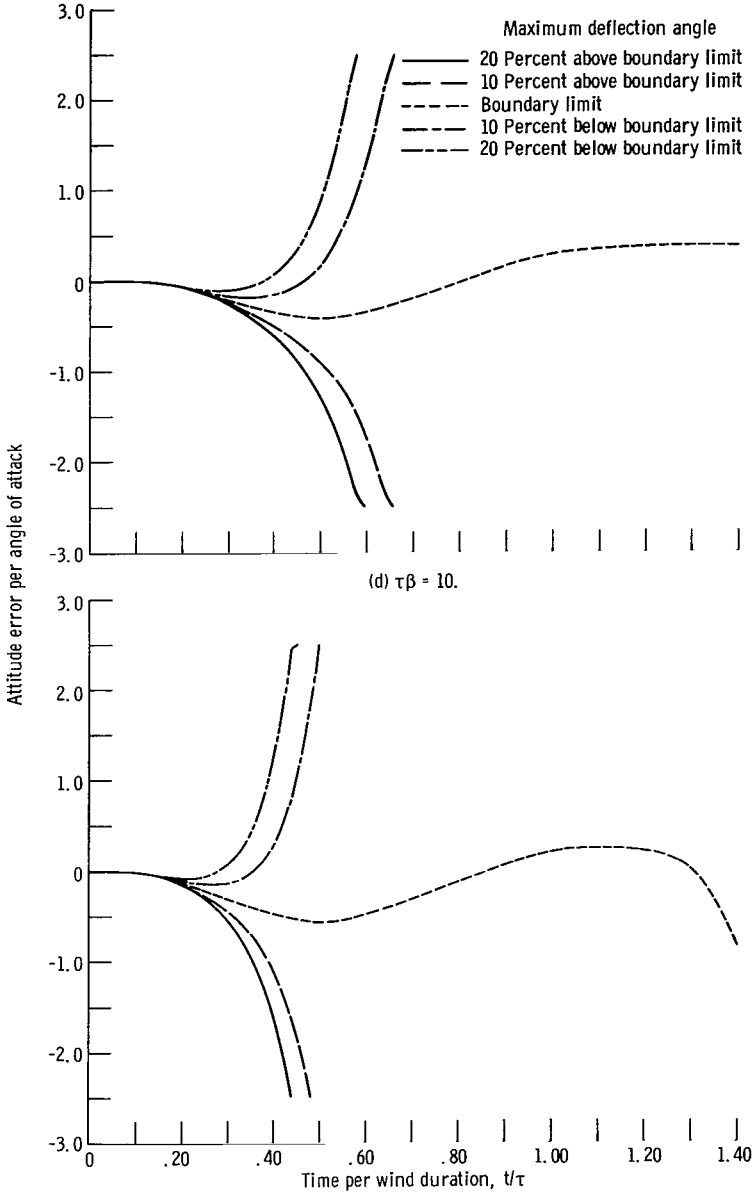

(d) $\tau\beta = 10$.

(e) $\tau\beta = 14$.

Figure 4. - Concluded.

Equation (13) is plotted in figures 3 and 4.

Optimum control. - It is shown in appendix C by the use of calculus of variations that, if the wind time history is given, the gimbal angle against time history, which gives the smallest peak absolute value of gimbal angle, is the one where $\delta - \delta_n$ is constant. For a wind starting at time zero and control action applied at $t = t_1$, using equation (6b), the optimum control is given by

$$\left(\delta - \delta_n\right)_{max} = -B\beta e^{\beta t_1} \int_0^\infty e^{-\beta t}\, \alpha_w\, dt$$

The factor $e^{\beta t_1}$ is the penalty for initiating a control action late, or the advantage that can be gained by starting early ($t_1 < 0$). The preceding equation gives the absolute minimum deflection that will maintain a stable flight.

General Stability Analysis

Appendix B develops the linearized differential equation for the flight-path angle. The resulting equations (B3) and (B6) form a complete set for the system. Combining the two equations results in equation (B8); that is,

$$\mathcal{L}(\Theta - \Theta_n) = -\frac{\frac{\beta^2}{B}}{s^2(s^2 - \beta^2)}\left[(s + b_1)\,\mathcal{L}(\delta - \delta_n) + B(s + b_2)\,\mathcal{L}(\alpha_w)\right] \tag{14}$$

Applying the boundary condition given by equation (4b) to equation (14) gives another important result of the analysis; that is,

$$\lim_{s \to \beta} \mathcal{L}(\delta - \delta_n) = -BK_1 \lim_{s \to \beta} \mathcal{L}(\alpha_w) \tag{15a}$$

where

$$K_1 = \frac{\beta + b_2}{\beta + b_1} < 1 \tag{15b}$$

Rectangular wind. - The wind profile and control action are assumed to be the same as in the previous section on rectangular wind. Using equation (15a), the boundary condition becomes

$$y_{BR} = K_1(1 - e^{-\tau\beta}) \tag{16}$$

This equation shows that the deflection requirement is reduced if changes in the flight path angle are included. This was expected because it represents the amount of sideslip caused by the disturbance, which tends to reduce the angle of attack and consequently the deflection requirement. The amount of reduction depends on the particular vehicle configuration, because β, b_1, and b_2 are functions of the configuration. Generally speaking the reduction in deflection requirement would not be enough to preclude using full trim control just as in the case of no γ effect, since $K_1 \simeq 1$. Attitude error convergence and divergence rates can be obtained in the same way as in the previous sections, by taking the inverse Laplace transform of equation (14).

Triangular wind. - The wind profile is assumed to be the same as in the previous section on triangular winds. Control action will also be the same; however, in this case, $\delta - \delta_n$ will include the flight-path angle change from the nominal. The control action is given by

$$\delta - \delta_n = \begin{cases} \delta_T - \delta_n & \text{for } 0 \leq t < a \\ \delta_{max} & \text{for } a \leq t \end{cases}$$

From equation (14)

$$\mathscr{L}(\delta_T - \delta_n) = -B\,\frac{s + b_2}{s + b_1}\,\mathscr{L}(\alpha_w)$$

In order to obtain the $\mathscr{L}(\delta - \delta_n)$, the inverse Laplace transform of the equation must first be evaluated. Then taking the Laplace transform of

$$\delta - \delta_n = [u(t) - u(t - a)](\delta_T - \delta_n) + \delta_{max}u(t - a)$$

gives

$$\mathscr{L}(\delta - \delta_n) = -\frac{B\alpha_{w,max}}{\frac{\tau}{2}}\left\{\frac{s + b_2}{s^2(s + b_1)} - \left[\frac{1}{s^2} - \frac{\tau}{2}y_{BR}(1 - K)\frac{1}{s} + \frac{b_2 - b_1}{b_1^2}\left(\frac{e^{-b_1 a}}{s + b_1} + \frac{b_1}{s^2} + \frac{b_1 a}{s} - \frac{1}{s}\right)\right] e^{-as}\right\} \tag{17}$$

Applying the boundary condition given by equation (15a) and triangular wind profile gives

$$\left[1 - \frac{\tau\beta}{2} y_{BR}(1 - K) + (b_2 - b_1)\left(\frac{\beta}{b_1}\right)^2\left(\frac{e^{-b_1 a}}{\beta + b_1} + \frac{b_1}{\beta^2} + \frac{b_1 a}{\beta} - \frac{1}{\beta}\right)\right] e^{-a\beta} = K_1 e^{-\tau\beta}(2e^{\tau\beta/2} - 1) \tag{18}$$

The results of equation (18) are plotted in figure 5 for 100- and 50-percent deflection dead bands. Results are presented for the two vehicle configurations discussed earlier

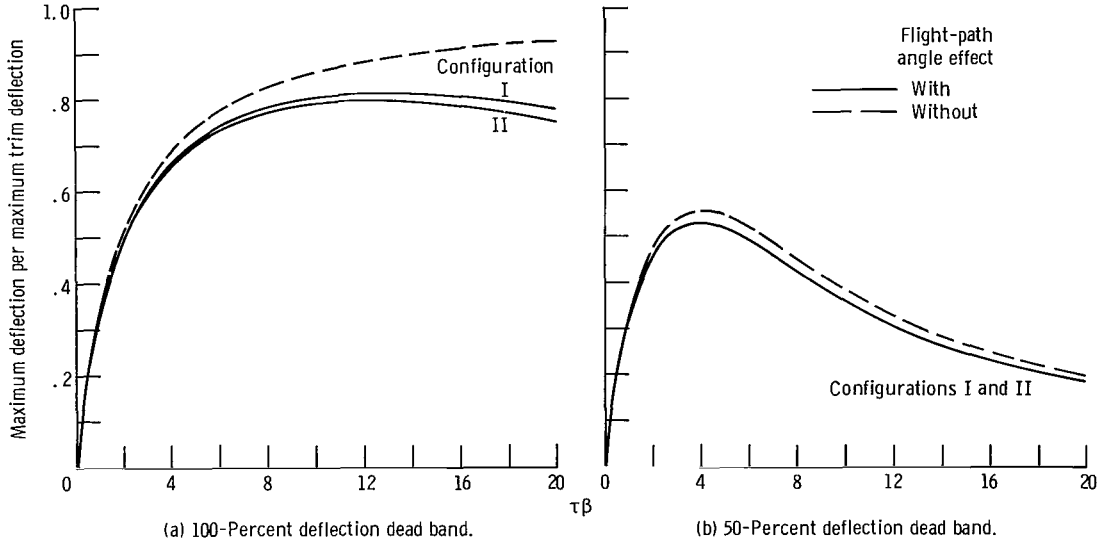

(a) 100-Percent deflection dead band. (b) 50-Percent deflection dead band.

Figure 5. - Theoretical stability boundary with and without flight-path angle effect for triangular wind.

and compared with the case without flight-path angle effect given in figure 5. As it was expected, the boundary limit is reduced by including the flight-path angle change. For the case of 100-percent deflection dead band and a $\tau\beta = 4$, the reduction is about 4 percent compared with the boundary with no flight-path angle included. The reduction is significant for larger values of $\tau\beta$.

The attitude response has been evaluated by taking the inverse transform of equation (14) with the appropriate deflection and wind profiles. The resultant equation is given in appendix B (eq. (B9)) and is plotted in figures 6 to 9. These figures are discussed in more detail in the RESULTS section.

Optimum control. - It is shown in appendix C that, for a given wind profile, the gimbal angle against time profile, which gives the smallest possible peak gimbal angle, is

the one in which $\delta - \delta_n = \pm\delta_{max}$. More specifically the optimal control function contains (N - 1) segments for which $\delta = \delta_{max}$ or $\delta = -\delta_{max}$, where N is the number of real pole locations of $\Theta - \Theta_n$ in the right half of the plane. It is also shown that, if one of the poles is much larger than the others (this is the case for the present problems), the minimum value of δ_{max} is nearly the same as for the single-pole case, except for triangular winds with large values of τ.

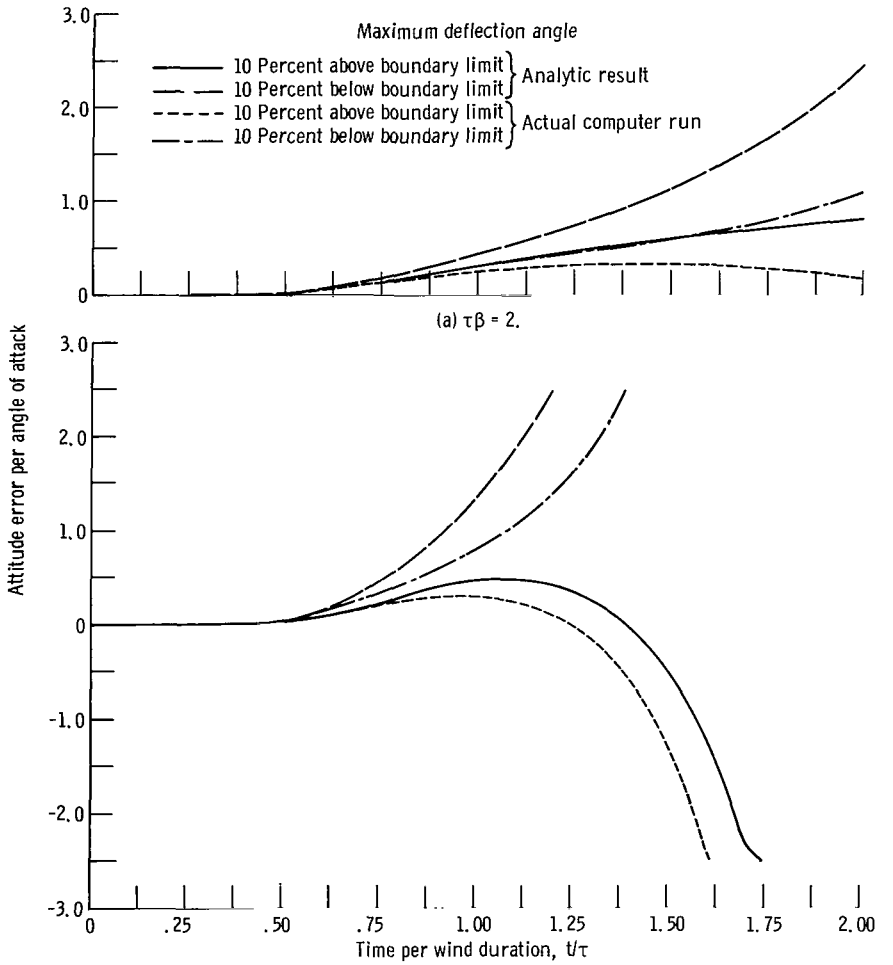

Figure 6. - Analytic and actual attitude error convergence and divergence rates for vehicle configuration I. Flight-path angle effect included; deflection dead band, 100 percent.

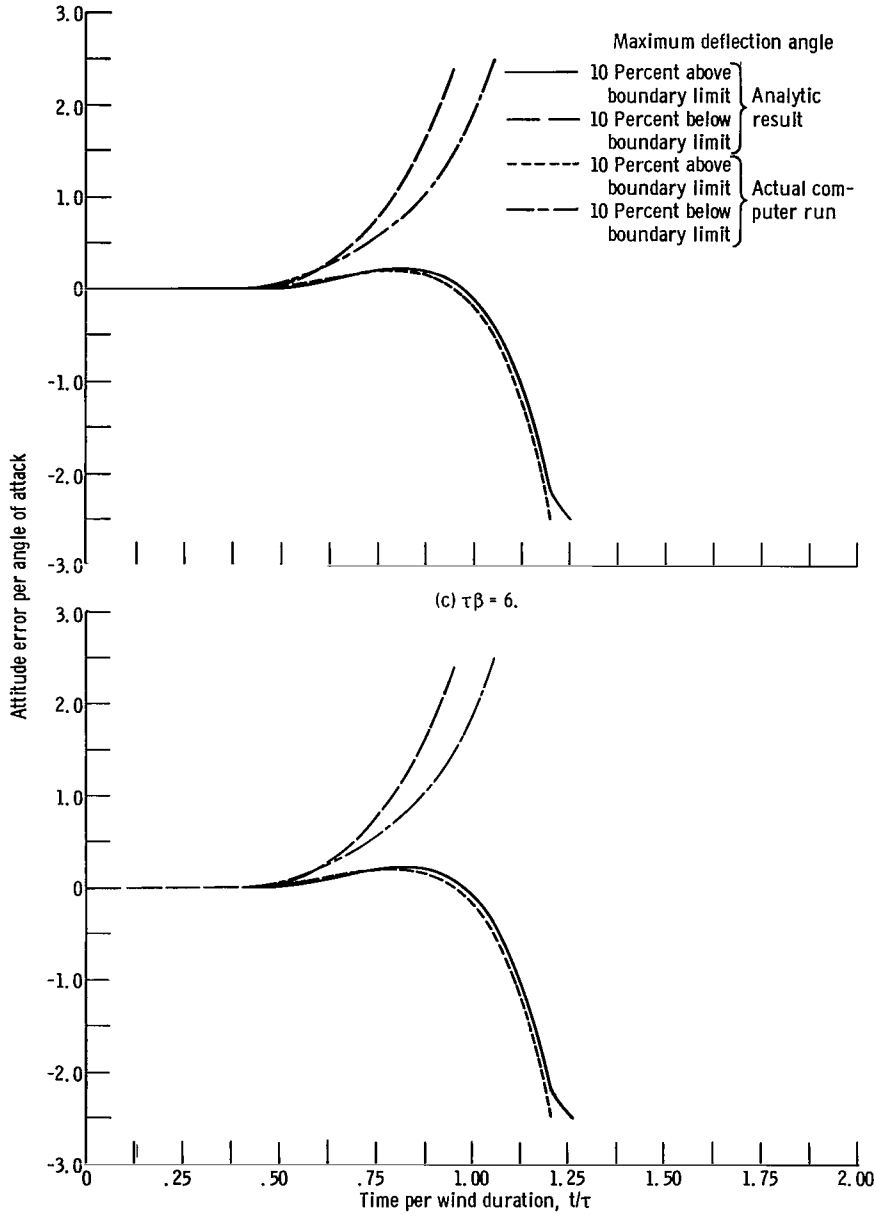

(c) $\tau\beta = 6$.

(d) $\tau\beta = 10$.

Figure 6. - Concluded.

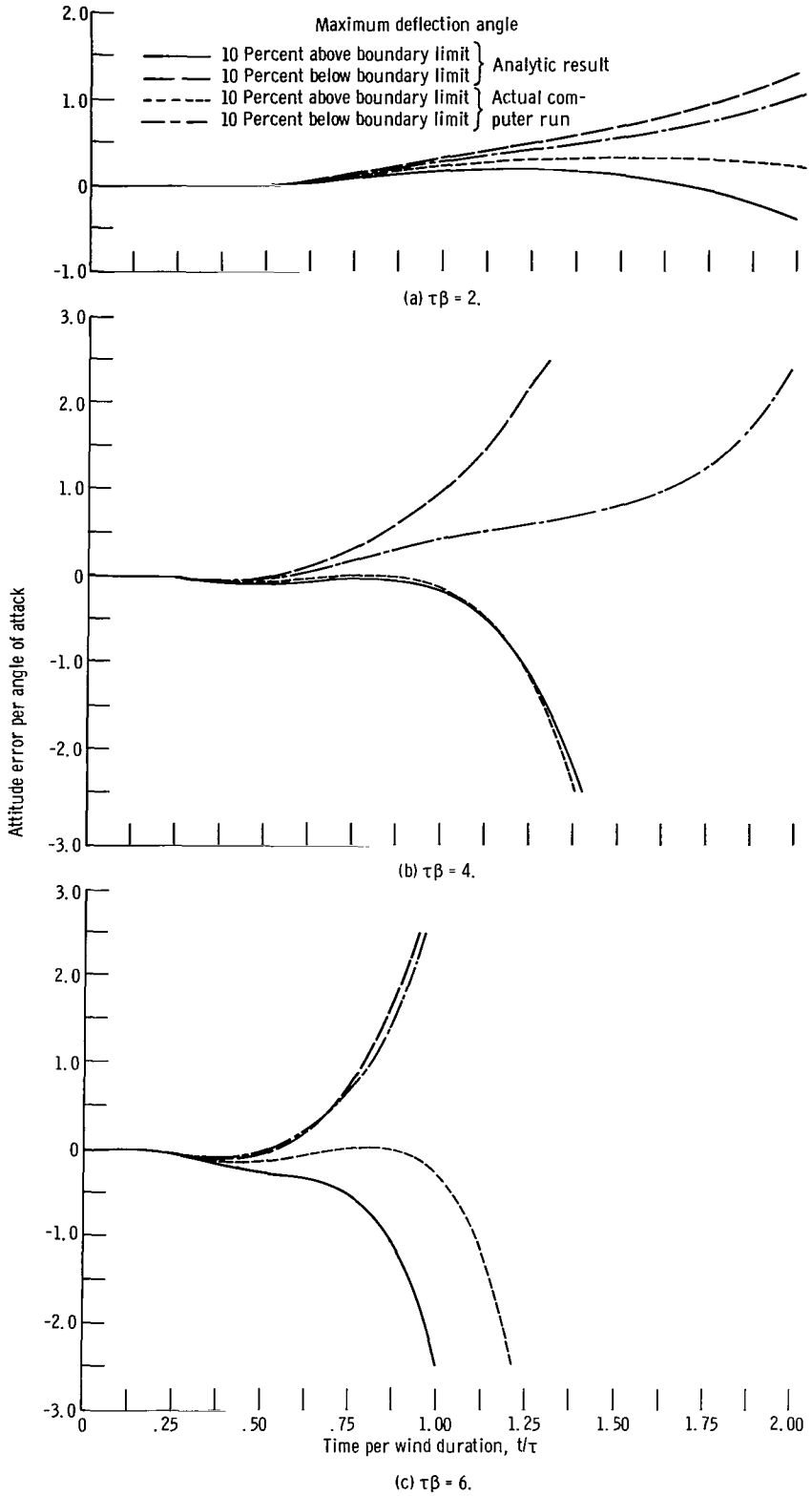

Figure 7. - Analytic and actual attitude error convergence and divergence rates for vehicle configuration I. Flight-path angle effect included; deflection dead band, 50 percent.

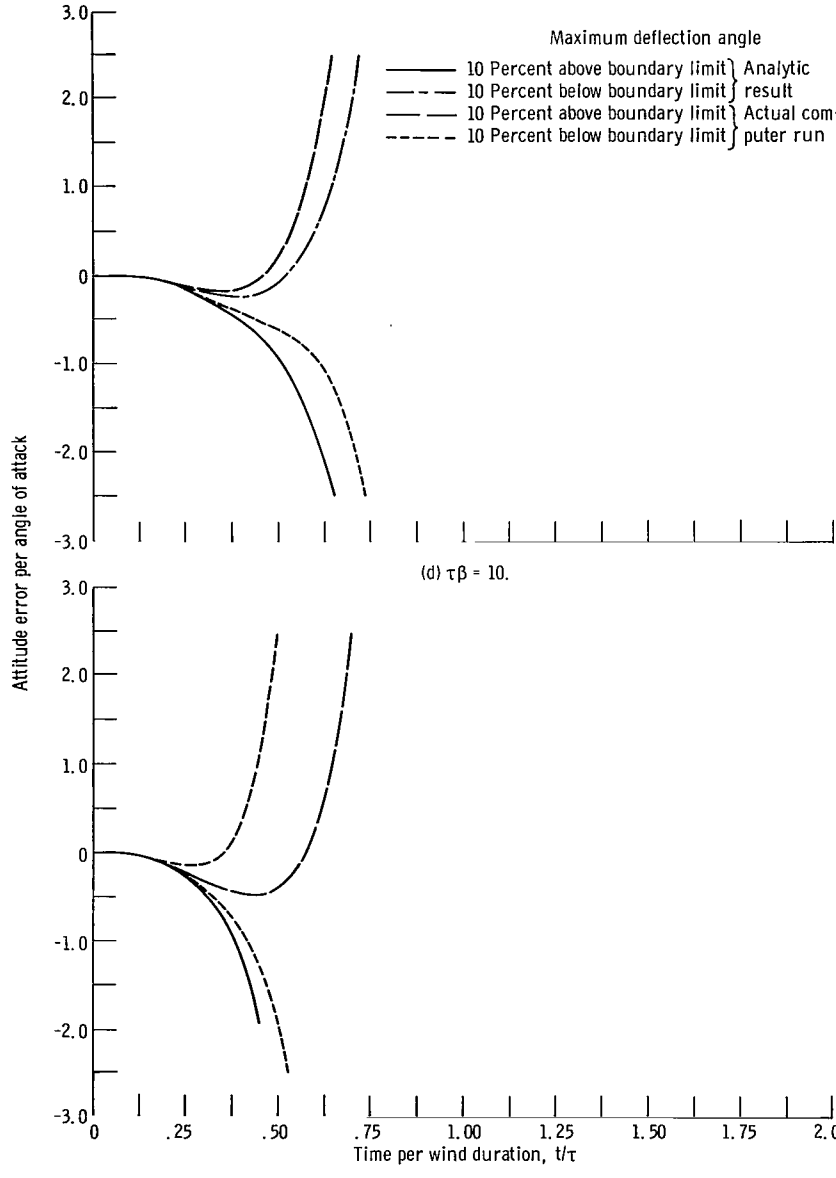

(d) $\tau\beta = 10$.

(e) $\tau\beta = 14$.

Figure 7. - Concluded.

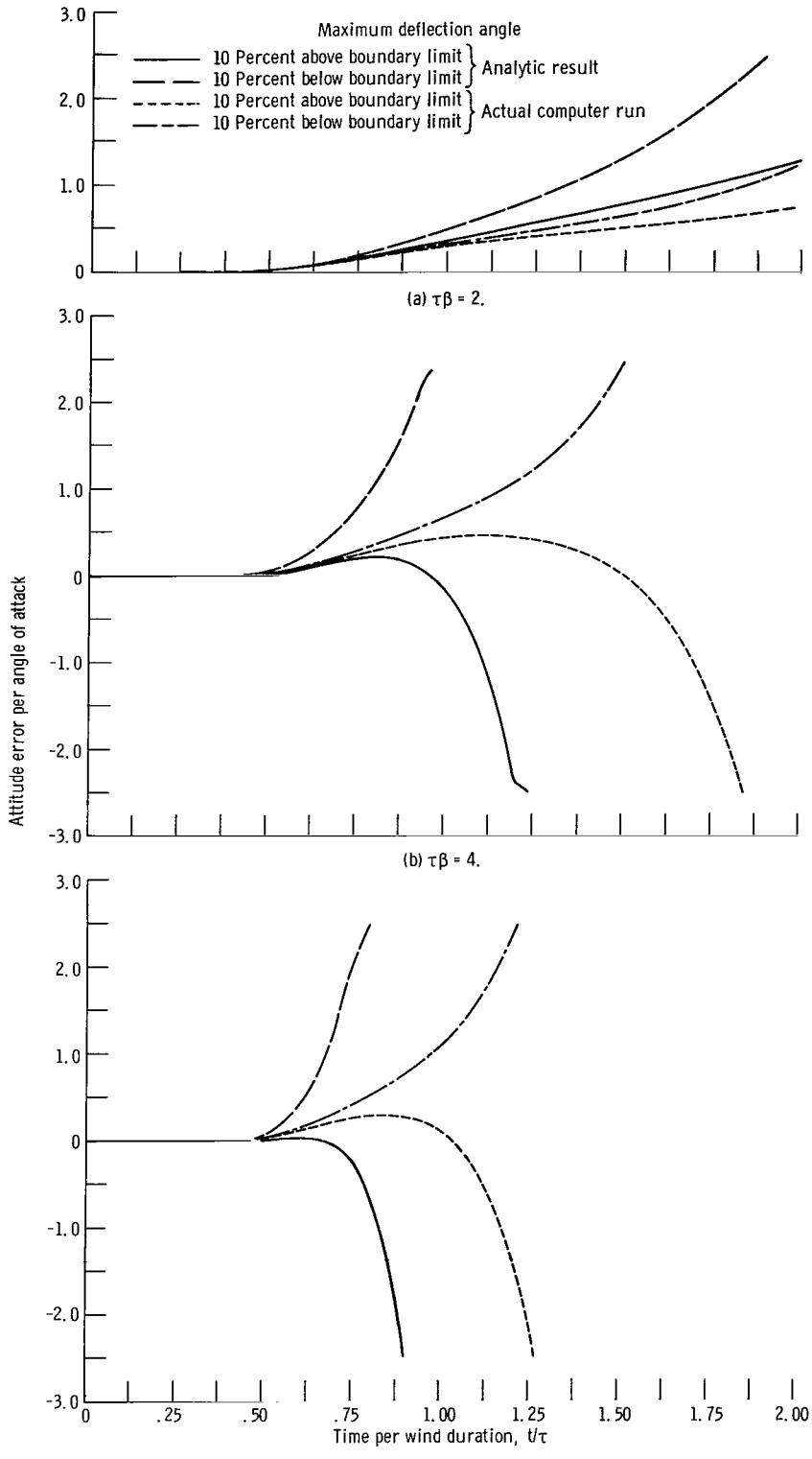

Figure 8. - Analytic and actual attitude error convergence and divergence rates for vehicle configuration II. Flight-path angle effect included; deflection dead band, 100 percent.

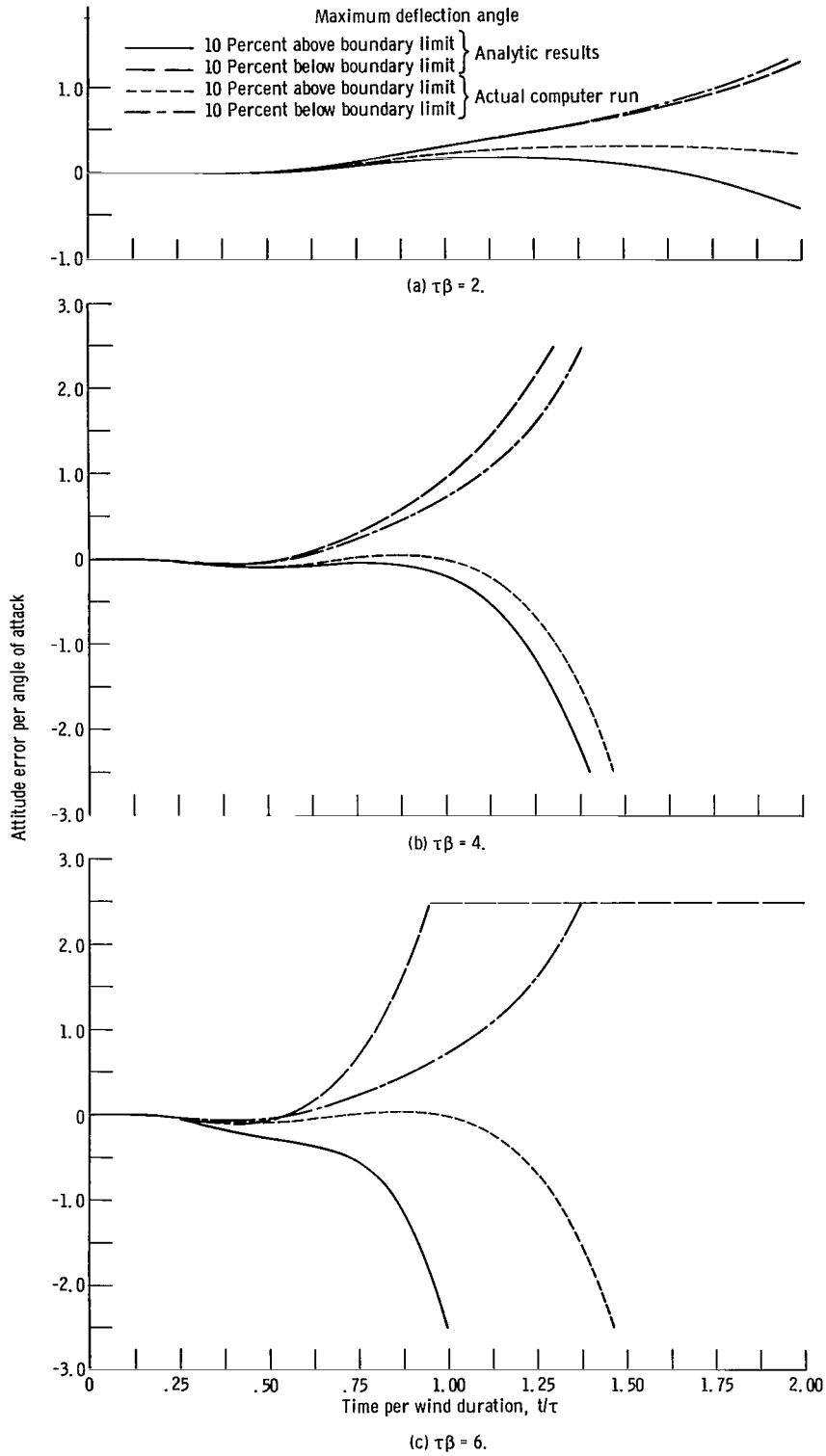

Figure 9. - Analytic and actual attitude error convergence and divergence rates for vehicle configuration II. Flight-path angle effect included; deflection dead band, 50 percent.

COMPUTER SIMULATION

To show the accuracy of previously obtained equations, a six degrees of freedom trajectory program was used to obtain actual stability boundaries. Computer simulations with detailed aerodynamic, propulsion, and inertia calculations were made for two vehicle configurations, the 260-inch (660-cm) solid booster (configuration I) and a large solid vehicle (configuration II) capable of delivering 1 million pounds (453 600 kg) of payload to 100-nautical-mile (184-km) orbit. Weight, inertia, and aerodynamic force coefficients have been generated at Lewis. Both vehicles were targeted to a 100-nautical-mile circular orbit with the constraint that the dynamic pressure will not exceed 950 pounds per square foot. The booster portion of flight, or aerodynamic flight, is constrained to a zero lift path to establish the nominal flight profile Θ_n, which was curve fitted for the nonnominal trajectory simulations. Pertinent trajectory and vehicle parameters used to obtain theoretical boundary values are given in table I for both configurations at maximum

TABLE I. - NOMINAL TRAJECTORY PARAMETERS AT MAXIMUM DYNAMIC PRESSURE

	Configuration	
	I	II
Weight, W, N	1.48×10^6	1.393×10^7
Moment of inertia, I, (kg)(m^2)	0.225×10^8	1.033×10^9
Normal force per angle of attack, N, N/rad	0.667×10^6	0.562×10^7
Total thrust, T, N	2.495×10^6	3.334×10^7
Aerodynamic moment arm, l_a, m	9.45	28.78
Control moment arm, l_c, m	23.56	50.27
Axial force, F_A, N	0.807×10^5	0.962×10^6
Nominal relative velocity, V_n, m/sec	538.81	614.23
Nominal flight attitude, Θ_n, deg	44.83	37.52
Time, t, sec	66	85

dynamic pressure conditions. Wind profiles correspond to those used in the analysis. Synthetic winds can be closely approximated by a triangle of appropriate time duration. Real winds are more difficult to approximate by rectangular or triangular shapes. However, reasonable results can be obtained by approximating the real wind with a triangle of the same area and maximum velocity.

The control system was programmed to apply trim control until the deflection required reached K percent of maximum, then use maximum allowable control.

RESULTS

Boundary values given by equations (8), (12), and (17) are plotted in figures 2 and 5. In figure 2, the percent of trim deflection required for stability is shown for rectangular and triangular wind profiles with no flight-path angle effects included. Boundary values for 100-, 75-, 50-, 25-, and 0-percent deflection dead bands are presented for triangular winds. As is seen from this figure, for rectangular wind profiles, the vehicle must be trimmed at all times, because 98 percent of trim deflection is needed to maintain stability for a typical value of $\tau\beta = 4$. For the same value of $\tau\beta$ in the case of triangular winds, only 69 percent of trim control requirement is needed for a 100-percent deflection dead band. This value can be further reduced by anticipating the wind to behave in a certain way. Obviously, if the wind velocity is assumed to continue to increase, the best control action would be to use maximum control capability as soon as the wind is observed. In this way, the control requirement can be reduced to 38 percent of trim value for zero-percent deflection dead band. This procedure defines the minimum control requirement attainable. Unfortunately, it requires accurate wind prediction.

A more realistic control procedure would be to trim the vehicle until the wind angle of attack exceeds some fixed limit, then apply maximum control. A 50-percent deflection dead band which is switching at half maximum control capability, reduces the deflection requirement to 56 percent of trim for $\tau\beta = 4$, or more for long wind duration. Figure 5 gives a comparison between boundary limits with and without flight path angle effects for different values of dead band. As was expected, there is large reduction in control requirements due to flight-path angle effect for long wind duration because of sideslip or drift velocity, which tends to reduce the angle of attack. In figure 5(a), for $\tau\beta = 4$, the reduction is about 4 percent, and it increases to 24 percent for $\tau\beta = 20$. Figure 5(b) is plotted for a deflection dead band of 50 percent, and the reduction in control requirement is negligible because the angle of attack is reduced and the sideslip is essentially eliminated.

The results given in figure 5(b) indicate that approximately 56 percent of trim control capability will maintain stability, although the vehicle will deviate from the nominal flight profile. The amount of attitude error, for triangular wind profiles and no flight-path angle effect included, may be obtained from figures 3 and 4, for different values of control dead band. The curves represent attitude error for control capability 10 and 20 percent above and below the boundary value. For the 260-inch (660-cm) solid-fueled rocket with $\beta = 0.53$ reciprocal second and a wind duration of 7.5 seconds, τ_β will equal 4. Assuming 100-percent deflection dead band and with a control capability 10 percent above the boundary, the maximum attitude error is 0.16° per wind angle of attack. For a 5° angle of attack, the vehicle attitude would deviate a maximum of 0.8° from the nominal. The attitude error goes to zero at $t/\tau \simeq 1$, or $t \simeq 7.5$ seconds. The attitude error continues in the negative direction after passing through zero. For the real auto-

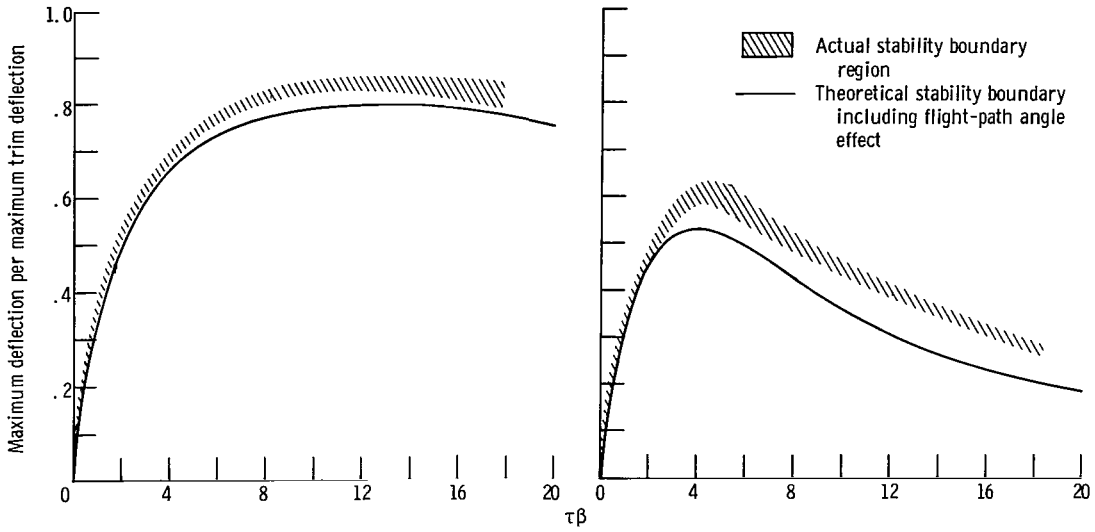

(a) 100-Percent deflection dead band.

(b) 50-Percent deflection dead band.

Figure 10. - Theoretical and actual stability boundary for vehicle configuration I.

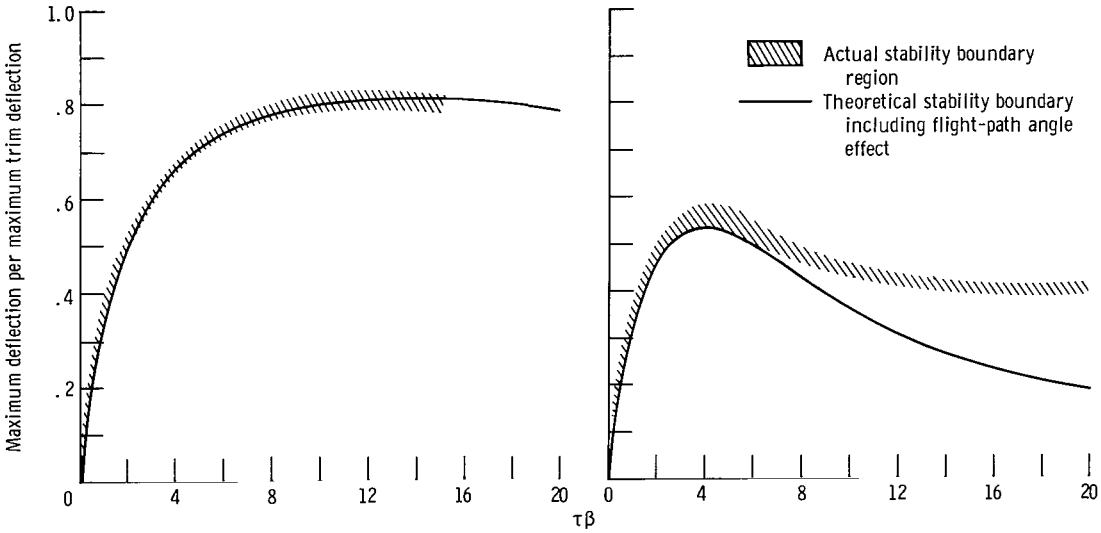

(a) 100-Percent deflection dead band.

(b) 50-Percent deflection dead band.

Figure 11. - Theoretical and actual stability boundary for vehicle configuration II.

pilot, however, the engine deflection would be decreased to the value required to maintain control after the attitude error has gone to zero. Therefore, the negative portions of figures 3 and 4, and 6 to 9 should be neglected as far as attitude error is concerned. The shape of these curves, however, give valuable information about the rate of convergence to the nominal attitude. The curves show rapid convergence and divergence rates above and below boundary value conditions, respectively. For triangular winds, the attitude error in most cases goes to zero before the wind subsides with a control capability 10 percent above boundary value. The exceptions are short wind gusts or rectangular wind distributions. In these cases, the time required to eliminate attitude errors is of the order of 1 to 2 times the wind duration.

Figures 10 and 11 give a comparison of actual and theoretical boundary limits for the two vehicle configurations. In both cases, there is good agreement with the actual six degrees of freedom computer simulations. In the analysis, it was assumed that the trajectory parameters will remain constant. However, in the actual flight they do vary, and their variations limit the time interval to which the theoretical results may be applied. This limitation could be partially circumvented by doing a point by point calculation along the trajectory with the appropriate wind for each segment. However, in general, it is sufficient to obtain deflection requirements at maximum aerodynamic load conditions.

A comparison of actual computer results and the theoretical results with flight-path angle included are given in figures 6 to 9. These figures show that the theoretical results are conservative; that is, the convergence rate is slower while the divergence rate is faster than the actual computer results.

CONCLUSIONS

The equations presented and the analytic results derived give a concise and complete description of an open-loop minimal control requirement to maintain stability for a general rigid-body vehicle configuration. The formulas are easily applicable, with the added advantage that the analysis can be carried out at any particular flight time. The results are given for the pitch plane, but, with minor modifications, they can also be applied to the yaw plane.

General stability boundary conditions are presented which do not depend on the vehicles considered in this report, and can be easily applied to any vehicle configuration by computing a single vehicle dependent parameter. It is also shown (for the vehicle configurations considered) that these boundary conditions give slightly conservative results. For more accurate results, several additional vehicle- and trajectory-dependent parameters must be calculated and a transcendental equation must be solved.

The results obtained show that, with good control-system design, the deflection requirements can be reduced to about 56 percent of trim deflection. At the same time, because of the method of control, the maximum angle of attack and bending moments can also be substantially reduced.

Rapid convergence and divergence rates are also shown for control capability above and below the given stability boundary, respectively. This implies rapid convergence to the nominal flight profile after deviation from it due to some disturbance, if the control capability is only slightly above the stability boundary value. Although the convergence rate is rapid, in designing a closed-loop control system one should not get too close to the boundary limit because, if the system becomes unstable for any reason, the divergence is also rapid.

A comparison of actual (detailed computer simulation) and theoretical attitude errors indicates that the theory gives somewhat conservative results; that is, the theoretical convergence rate is slower while the divergence rate is faster than the actual.

Lewis Research Center,
National Aeronautics and Space Administration,
Cleveland, Ohio, January 31, 1968,
125-17-05-01-22.

APPENDIX A

SYMBOLS

a	control switching time defined by eq. (10), sec
B	constant defined by eq. (2)
b_1, b_2	constants defined in appendix B, sec^{-1}
C_i	constants defined in appendix B, sec^i
$dc_n/d\alpha$	normal force coefficient per angle of attack, rad^{-1}
D_i	defined in eq. (C1)
E	Wierstrass E variable
F_A	axial force, N
f_i	constraint equations defined in appendix C
g	gravitational acceleration, m/sec^2
I	moment of inertia, $(kg)(m^2)$
J	function to be minimized defined in appendix C
K	multiplier (percent deflection dead band)
K_1	constant defined by eq. (16)
l_a	aerodynamic moment arm, m
l_c	control moment arm, m
M_{cg}	total moment about center of gravity, N
m	gross mass, kg
N	normal force per angle of attack, N/rad
S	vehicle base area, m^2
s	Laplace variable, sec^{-1}
T	total thrust, N
t	time, sec
t_s	switching time defined in appendix C, sec
u(t)	unit step function
V	relative velocity including wind, m/sec
V_R	relative velocity, m/sec
V_w	wind velocity, m/sec
W	gross weight, N
y_{BR}	boundary limit
α	angle of attack, rad
α_w	wind angle of attack, rad
β	vehicle response parameter, sec^{-1}
β_i	unstable roots, sec^{-1}
γ	flight path angle, rad
δ	deflection angle, rad
Θ	flight attitude, rad
λ_i	undetermined Lagrange multipliers
ρ	air density, kg/m^3
σ	real variable defined in appendix C
τ	wind duration, sec

Subscripts:

max	maximum
n	nominal
T	trim

APPENDIX B

EQUATIONS OF MOTION

The basic vehicle equations of motion will be derived for a rigid-body configuration. Only motion in the pitch plane is considered. The equations of motion and the vehicle's control system are treated as uncoupled, insofar as the vehicle's three axes of rotation are concerned. The equations are given in the pitch plane, but the yaw plane analysis can be done in a similar fashion. In order to apply the following equations to the yaw plane, the only changes that have to be made are to set $\Theta_n = 90^o$ and $g \cos \Theta_n / V_n = 0$ in equation (4). The basic vehicle configuration is given in figure 1, and the reader is referred to appendix A for the definition of variables and symbols used.

Basic equations of motion:

$$\sum F_{\parallel V} = m\dot{V} = T \cos (\Theta - \gamma + \delta) - F_A \cos (\Theta - \gamma) - N\alpha \sin (\Theta - \gamma) - W \sin \gamma \tag{B1a}$$

$$\sum F_{\perp V} = mV\dot{\gamma} = T \sin (\Theta - \gamma + \delta) - F_A \sin (\Theta - \gamma) + N\alpha \cos (\Theta - \gamma) - W \cos \gamma \tag{B1b}$$

$$\sum M_{CG} = I\ddot{\Theta} = N l_a \alpha - T l_c \sin \delta \tag{B1c}$$

$$N = \frac{1}{2} \rho V_R^2 \frac{dc_n}{d\alpha} S \tag{B1d}$$

$$\sin \alpha_w = \frac{V_w}{V_R} \sin \gamma \tag{B1e}$$

$$\alpha = \Theta - \gamma - \alpha_w \tag{B1f}$$

Using small-angle approximations for α, α_w, and δ, the equations become

$$\sum F_{\parallel V} = m\dot{V} = T \left[\cos (\Theta - \gamma) - \delta \sin (\Theta - \gamma)\right] - F_A \cos (\Theta - \gamma) - N\alpha \sin (\Theta - \gamma) - W \sin \gamma \tag{B2a}$$

$$\sum F_{\perp V} = mV\dot{\gamma} = T \left[\sin (\Theta - \gamma) + \delta \cos (\Theta - \gamma)\right] - F_A \sin (\Theta - \gamma) + N\alpha \cos (\Theta - \gamma) - W \cos \gamma \tag{B2b}$$

$$\sum M_{CG} = I\ddot{\Theta} = N l_a \alpha - T l_c \delta \tag{B2c}$$

$$\alpha_w = \frac{V_w}{V_R} \sin \gamma \tag{B2d}$$

$$\alpha = \Theta - \gamma - \alpha_w \tag{B2e}$$

To derive the principal analytic results of this report, it is necessary to express the attitude error in terms of the wind and control action. The attitude error is given by $\Theta - \Theta_n$ or, from equation (B2c),

$$I(\ddot{\Theta} - \ddot{\Theta}_n) = N l_a(\alpha - \alpha_n) - T l_c(\delta - \delta_n)$$

Substituting for $(\alpha - \alpha_n)$ from equation (B2e) into the preceding equation and taking the Laplace transform give

$$\mathcal{L}(\Theta - \Theta_n) = -\frac{\beta^2}{s^2 - \beta^2} \left\{ \mathcal{L}(\gamma - \gamma_n) + \frac{1}{B} \left[\mathcal{L}(\delta - \delta_n) + B\,\mathcal{L}(\alpha_w) \right] \right\} \tag{B3}$$

where

$$\beta^2 = \frac{N l_a}{I} \qquad B = \frac{N l_a}{T l_c} \tag{B4}$$

In order to eliminate $\mathcal{L}(\gamma - \gamma_n)$ from equation (B3), equations (B1a) and (B1b) must be linearized about some nominal operating point.

Linearized equations for the flight-path angle. - In the following analysis, the same symbols will be used for the linearized variables as for the actual variables. Keeping the same symbols simplifies the notations and makes the equations less confusing. Linearizing equations (B2a) and (B2b) gives

$$m\dot{V} = -T \sin(\Theta - \gamma + \delta)_n(\Theta - \gamma + \delta) + F_A \sin(\Theta - \gamma)_n(\Theta - \gamma) - N\alpha_n \cos(\Theta - \gamma)_n(\Theta - \gamma)$$

$$- W \cos \gamma_n \gamma - N\alpha \sin(\Theta - \gamma)_n$$

$$m(V\dot{\gamma}_n + V_n\dot{\gamma}) = T\cos(\Theta - \gamma + \delta)_n(\Theta - \gamma + \delta) - F_A\cos(\Theta - \gamma)_n(\Theta - \gamma)$$

$$- N\alpha_n \sin(\Theta - \gamma)_n(\Theta - \gamma) + N\alpha\cos(\Theta - \gamma)_n + W\sin\gamma_n\gamma$$

but $\delta_n << \Theta_n$, $\alpha_n = 0$, and $\Theta_n = \gamma_n$; therefore,

$$m\dot{V} = -W\cos\Theta_n\gamma$$

$$m(V\dot{\gamma}_n + V_n\dot{\gamma}) = T(\Theta - \gamma + \delta) - F_A(\Theta - \gamma) + N\alpha + W\sin\Theta_n\gamma$$

Substituting for V_n and $\dot{\gamma}_n$ from equations (B1a) and (B1b) and taking the Laplace transform give

$$\mathcal{L}(\gamma) = \frac{1}{mV_n}\frac{s}{s^2 + \dfrac{T - F_A - W\sin\Theta_n}{mV_n}s + \left(\dfrac{g\cos\Theta_n}{V_n}\right)^2}\mathcal{L}\left[(T - F_A)\Theta + T\delta + N\alpha\right]$$

Substituting for α from equation (B2e) gives

$$\mathcal{L}(\gamma) = \frac{1}{mV_n}\frac{s\mathcal{L}\left[(T - F_A + N)\Theta + T\delta - N\alpha_w\right]}{s^2 + \dfrac{T - F_A + N - W\sin\Theta_n}{mV_n}s + \left(\dfrac{g\cos\Theta_n}{V_n}\right)^2} \tag{B5}$$

Because

$$\left(\frac{g\cos\Theta_n}{V_n}\right)^2 << \frac{T - F_A + N - W\sin\Theta_n}{mV_n}|s|$$

there are two real roots, one of which is located very close to the origin. To simplify the analysis, the smaller root is assumed to be at the origin. Then

$$\mathcal{L}(\gamma) = \frac{1}{mV_n}\frac{1}{s + C_1}\mathcal{L}\left[(T - F_A + N)\Theta + T\delta - N\alpha_w\right] \tag{B6}$$

where

$$C_1 = \frac{T - F_A + N - W \sin \Theta_n}{mV_n}$$

Substituting equation (B6) into equation (B3) gives

$$\mathcal{L}(\Theta - \Theta_n) = -\frac{\beta^2}{\frac{B}{P(s)}}\left[(s + b_1)\mathcal{L}(\delta - \delta_n) + B(s + b_2)\mathcal{L}(\alpha_w)\right]$$

where

$$P(s) = s^3 + C_1 s^2 - \beta^2 s + C_2$$

$$C_2 = \beta^2 \frac{g \sin \Theta_n}{V_n}$$

$$b_1 = \frac{1}{mV_n}\left[T - F_A + N\left(1 + \frac{l_a}{l_c}\right) - W \sin \Theta_n\right] \tag{B7}$$

$$b_2 = \frac{1}{mV_n}(T - F_A - W \sin \Theta_n)$$

Since C_1 and C_2 are much smaller than β^2, the polynomial P(s) can be factored as

$$P(s) = \left(s - \frac{C_2}{\beta^2}\right)\left[s^2 + \left(C_1 + \frac{C_2}{\beta^2}\right)s - \beta^2\right]$$

Also, $|s|\left[C_1 + (C_2/\beta^2)\right] << \beta^2$ and the two roots are located at $s \approx \pm\beta$. The root C_2/β^2 is very small $\left[(C_2/\beta^2) \approx 0.01\right]$ and can be assumed to be zero. With these assumptions P(s) becomes

$$P(s) \approx s(s^2 - \beta^2)$$

therefore,

$$\mathcal{L}(\Theta - \Theta_n) = -\frac{\frac{\beta^2}{B}}{s(s^2 - \beta^2)}\left[(s + b_1)\mathcal{L}(\delta - \delta_n) + B(s + b_2)\mathcal{L}(\alpha_w)\right] \tag{B8}$$

The inverse Laplace transform of the attitude error response to triangular wind and trim deflection profile with dead band is given as follows:

$$\frac{\Theta - \Theta_n}{-\alpha_{w,\max}} = \frac{2}{\tau\beta}\left[\left\{\left[1 + a(b_2 - b_1) - \frac{b_1\tau}{2}Y_{BR}(1 - K)\right]\left[\sinh\tau\beta\left(\frac{t}{\tau} - \frac{a}{\tau}\right) - \tau\beta\left(\frac{t}{\tau} - \frac{a}{\tau}\right)\right]\right.\right.$$

$$+\frac{b_2}{\beta}\left[\cosh\tau\beta\left(\frac{t}{\tau} - \frac{a}{\tau}\right) + \frac{(\tau\beta)^2}{2}\left(\frac{t}{\tau} - \frac{a}{\tau}\right)^2 - 1\right] + \left[\frac{B(b_2 - b_1)}{b_1^2}\,e^{-b_1 a} + ab_1 - 1\right.$$

$$\left.\left.-\frac{\tau\beta}{2}Y_{BR}(1 - K)\right]\left[\cosh\tau\beta\left(\frac{t}{\tau} - \frac{a}{\tau}\right) - 1\right]\right\}u\left(\frac{t}{\tau} - \frac{a}{\tau}\right) - 2\left\{\sinh\tau\beta\left(\frac{t}{\tau} - \frac{1}{2}\right) - \tau\beta\left(\frac{t}{\tau} - \frac{1}{2}\right)\right.$$

$$+\frac{b_2}{\beta}\left[\cosh\tau\beta\left(\frac{t}{\tau} - \frac{1}{2}\right) - \frac{(\tau\beta)^2}{2}\left(\frac{t}{\tau} - \frac{1}{2}\right)^2 - 1\right]\Big\}u\left(\frac{t}{\tau} - \frac{1}{2}\right) + \left\{\sinh\tau\beta\left(\frac{t}{\tau} - 1\right) - \tau\beta\left(\frac{t}{\tau} - 1\right)\right.$$

$$\left.\left.+\frac{b_2}{\beta}\left[\cosh\tau\beta\left(\frac{t}{\tau} - 1\right) - \frac{(\tau\beta)^2}{2}\left(\frac{t}{\tau} - 1\right)^2 - 1\right]\right\}u\left(\frac{t}{\tau} - 1\right)\right] \tag{B9}$$

APPENDIX C

EQUATIONS FOR OPTIMUM CONTROL

The problem of finding the optimum deflection profile for a predictable wind profile can be stated mathematically as follows. It is desired to find the function $\delta(t)$, with the smallest possible maximum value, that satisfies a set of definite integral constraints. The constraints are given by equation (15a)

The problem is formulated mathematically as a Bolza problem of the calculus of variations; namely, it is desired to minimize δ_{max}, where δ_{max} is the maximum value of $\delta(t)$ subject to the following constraints:

$$f_i = \int_0^\infty e^{-\beta_i t}\, \delta(t)dt + BK_1 \int_0^\infty e^{-\beta_i t}\, \alpha_w(t)dt$$

$$= \int_0^\infty e^{-\beta_i t}\, \delta(t)dt - D_i \qquad i = 1, 2, 3, \ldots, N \tag{C1}$$

δ_{max} is defined by the additional constraint

$$f_{N+1} = \delta^2 - \delta_{max}^2 + \sigma^2 = 0 \tag{C2}$$

where σ is a real variable. The constraint equations are now adjoined to the function to be minimized in the usual manner, thus the function to be minimized J is

$$J = \sum_{i=1}^{N+1} \lambda_i f_i + \delta_{max}$$

where the λ_i are the undetermined LaGrange multipliers. The Euler-LaGrange equations to determine the optimum solution are

$$\frac{d}{dt}\left(\frac{\partial J}{\partial \dot{X}_i}\right) = \frac{dJ}{dX_i} \qquad i = 1, 2, \ldots, N$$

where

$$X_1 = \delta$$

$$X_2 = \sigma$$

Then

$$\sum_{i=1}^{N} \lambda_i e^{-\beta_i t} + 2\lambda_{N+1}\delta = 0 \tag{C3a}$$

$$2\lambda_{N+1}\sigma = 0 \tag{C3b}$$

From equation (C3a)

$$\delta = -\frac{1}{2\lambda_{N+1}} \sum_{i=1}^{N} \lambda_i e^{-\beta_i t}$$

In order for δ to be bounded, λ_{N+1} must not be zero. Therefore, from equation (C3b), σ must be equal to zero. Using this result and equation (C2) gives

$$\delta = \pm\delta_{max} \tag{C4}$$

The choice of sign in equation (C4) is determined by the Wierstrass E-test, which gives

$$E = J(\overline{X}^*) - J(\overline{X}) + \frac{\partial J}{\partial \dot{\overline{X}}}(\dot{\overline{X}} - \dot{\overline{X}}^*) \geq 0$$

for a minimum. For this problem

$$E = \sum_{i=1}^{N} \lambda_i e^{-\beta_i t}(\delta^* - \delta)$$

where δ is the minimum value and δ^* the allowable variation; in this case, $\delta^* = -\delta$. Then

$$2\sum_{i=1}^{N} \lambda_i e^{-\beta_i t} \delta \leq 0$$

Because the λ_i are constants, the preceding function can have at most N - 1 zeros. These zeros correspond to the switching points from $\delta = \delta_{max}$ to $\delta = -\delta_{max}$, and

$$\delta = \delta_{max} \quad \text{if} \quad \sum_{i=1}^{N} \lambda_i e^{-\beta_i t} \leq 0$$

$$\delta = -\delta_{max} \quad \text{if} \quad \sum_{i=1}^{N} \lambda_i e^{-\beta_i t} > 0$$

Example: Suppose there are two integral constraints. Then the switching function becomes

$$\lambda_1 e^{-\beta_1 t_s} + \lambda_2 e^{-\beta_2 t_s}$$

which gives a switching time of

$$t_s = -\frac{1}{\beta_2 - \beta_1} \ln\left(-\frac{\lambda_1}{\lambda_2}\right)$$

The solution is obtained by choosing δ_{max} and t_s such that equation (C1) is satisfied.

$$\delta_{max}\left(1 - 2e^{-\beta_1 t_s}\right) = \beta_1 D_1$$

$$\delta_{max}\left(1 - 2e^{-\beta_2 t_s}\right) = \beta_2 D_2$$

Combining these equations gives

$$\delta_{max} = \frac{\beta_2 D_2}{1 - 2e^{-\beta_2 t_s}} \qquad \text{(C5a)}$$

$$2e^{-\beta_1 t_s} - \frac{2\beta_1 D_1}{\beta_2 D_2} e^{-\beta_2 t_s} = 1 - \frac{\beta_1 D_1}{\beta_2 D_2} \tag{C5b}$$

Let

$$x = e^{-\beta_2 t_s}$$

$$y = \frac{\beta_1 D_1}{\beta_2 D_2}$$

Then equation (C5b) becomes

$$2x^{\beta_1/\beta_2} - 2xy = 1 - y \tag{C6}$$

If x is approximately zero or one, then equation (C5a) shows that the stability boundary is nearly unchanged from the single-pole solution. For most launch vehicles, β_2 is at least a factor of 10 larger than β_1. If this is the case, the solution to equation (C6) for $0 \leq y \leq 1$ is

$$x = \left(\frac{1 - y}{2}\right)^{\beta_2/\beta_1} \tag{C7}$$

Therefore, for $0 \leq y \leq 1$, x is never larger than 0.001. For $y = 1$, equation (C6) has two solutions: $x = 0$ or $x = 1$. The two solutions correspond to $t_s = 0$ or $t_s = \infty$ and $\delta_{max} = \beta_2 D_2$, and are, therefore, physically equivalent. For $y \gg 1$, the solution to equation (C6) has the form

$$x \simeq \frac{y - 1}{2y}$$

The total solution of equation (C6) is shown in sketch (c)

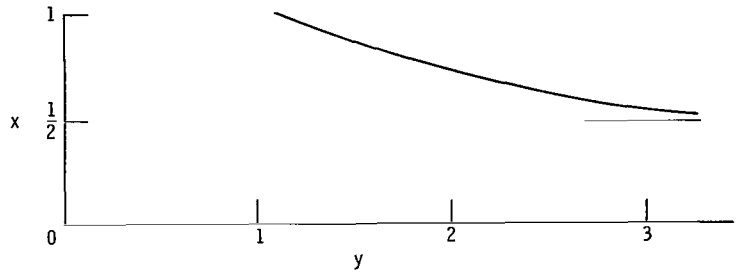

(c)

From the preceding discussion and sketch, the single-pole stability boundary solution can be expected to be valid up to $y = 1$. The value of y must now be related to τ for triangular winds, in order to predict the range of validity of the single-pole solution.

For a triangular wind duration τ,

$$D_i = \frac{1}{\beta_i^2}\left(1 - e^{-\tau\beta_i/2}\right)^2 \qquad i = 1, 2$$

and

$$y = \frac{\beta_2}{\beta_1}\left(\frac{1 - e^{-\tau\beta_1/2}}{1 - e^{-\tau\beta_2/2}}\right)^2 \tag{C8}$$

In the limit as τ approaches zero, y approaches β_1/β_2, which is less than 0.1. As τ approaches ∞, y goes to β_2/β_1, or at least 10. Therefore, there exists some value of τ at which $y = 1$. From equation (C8), the solution can be expressed as

$$e^{-\tau\beta_1/2} \cong 1 - \sqrt{\frac{\beta_1}{\beta_2}} \tag{C9}$$

If $\beta_2 = 0.5$ and $\beta_1 = 0.01$ (the approximate value for the vehicles considered herein), then $\tau \cong 28$ seconds for $y = 1$. Thus, the single-pole approximation can be expected to be valid up to $\tau = 28$ seconds (or $\tau\beta = 14$) for a triangular wind. For longer wind duration, the value of δ_{max} may increase substantially.

REFERENCE

1. Dawson, R. P.: Saturn IB Improvement Study (Solid First Stage), Phase II, Final Detailed Report. Rep. No. SM-51896, Vol. 2 (NASA CR-77129), Douglas Aircraft Co., Inc., Mar. 30, 1966.

NASA-Langley, 1968 —— 21 E-4297

"The aeronautical and space activities of the United States shall be conducted so as to contribute . . . to the expansion of human knowledge of phenomena in the atmosphere and space. The Administration shall provide for the widest practicable and appropriate dissemination of information concerning its activities and the results thereof."

—NATIONAL AERONAUTICS AND SPACE ACT OF 1958

NASA SCIENTIFIC AND TECHNICAL PUBLICATIONS

TECHNICAL REPORTS: Scientific and technical information considered important, complete, and a lasting contribution to existing knowledge.

TECHNICAL NOTES: Information less broad in scope but nevertheless of importance as a contribution to existing knowledge.

TECHNICAL MEMORANDUMS: Information receiving limited distribution because of preliminary data, security classification, or other reasons.

CONTRACTOR REPORTS: Scientific and technical information generated under a NASA contract or grant and considered an important contribution to existing knowledge.

TECHNICAL TRANSLATIONS: Information published in a foreign language considered to merit NASA distribution in English.

SPECIAL PUBLICATIONS: Information derived from or of value to NASA activities. Publications include conference proceedings, monographs, data compilations, handbooks, sourcebooks, and special bibliographies.

TECHNOLOGY UTILIZATION PUBLICATIONS: Information on technology used by NASA that may be of particular interest in commercial and other non-aerospace applications. Publications include Tech Briefs, Technology Utilization Reports and Notes, and Technology Surveys.

Details on the availability of these publications may be obtained from:

SCIENTIFIC AND TECHNICAL INFORMATION DIVISION

NATIONAL AERONAUTICS AND SPACE ADMINISTRATION

Washington, D.C. 20546